Defects in Highly Neutron Irradiated Graphite

***R. Mittal[1,2], M.K. Gupta[1], S.K. Mishra[1], S. Wajhal[1],H.K. Poswal[3], B.Singh[1,2], A.B. Shinde[1], P.S. Rama Krishna[1], Peram Delli Babu[4], Ratikant Mishra[2,5], Pulya Umamaheswara Sastry[1,2], Rakesh Ranjan[6] and Samrath Lal Chaplot[1,2]**

[1]Solid State Physics Division, Bhabha Atomic Research Centre, Mumbai, 400085, India
[2]Homi Bhabha National Institute, Anushaktinagar, Mumbai 400094
[3]High Pressure & Synchrotron Radiation Physics Division, Bhabha Atomic Research Centre, Trombay, Mumbai 400 085
[4]UGC-DAE Consortium for Scientific Research, Mumbai Centre, R5-Shed, BARC, Trombay, Mumbai - 400 085
[5]Chemistry Division, Bhabha Atomic Research Centre, Mumbai, 400085
[6]Reactor Operations Division, Bhabha Atomic Research Centre, Mumbai, 400085

Abstract

Graphite has been used as neutron moderator or reflector in many nuclear reactors. The irradiation of graphite in a nuclear reactor results in a complex population of defects. Heating of the irradiated graphite at high temperatures results in annihilation of the defects with release of an unusually large energy, called the Wigner energy. From various experiments on highly irradiated graphite samples from CIRUS reactor at Trombay and ab-initio simulations, we have for the first time identified various 2-, 3- and 4-coordinated topological structures in defected graphite, and provided microscopic mechanism of defect annihilation on heating and release of the Wigner energy. The annihilation process involves cascading cooperative movement of atoms in multiple steps involving an intermediate structure. Our work provides new insights in understanding of the defect topologies and annihilation in graphite which is of considerable importance to wider areas of graphitic materials including graphene and carbon nanotubes.

Keywords: Graphite, Neutron irradiation, Wigner energy, Ab-initio simulations, Annihilation of defects, Neutron diffraction

Introduction

Graphite has been used in high radiation environment, as neutron moderator or reflector, in many nuclear reactors, especially research and material testing reactors such as X-10 at Oak Ridge National Laboratory (USA), the Windscale Piles (UK) and G1 (Marcoule, France). About 250 kilo-tons of irradiated graphite inventory is present all over the world[1]. There is high interest in understanding of the change in behaviour of graphite, as well as in other graphitic materials such as graphene and carbon nanotubes due to irradiation[2,3]. The hexagonal structure of graphite[4] has layers of carbon atoms formed by strong covalent bonding in the a-b plane. These layers are stacked along the hexagonal axis and are held by van der Waals forces. The irradiation of graphite in a nuclear reactor results in the knocking out of carbon atoms from their equilibrium sites. Defects in graphite are unusual since they involve very large potential energy and are prevented from annealing at ambient or moderately high temperatures due to a large energy barrier. Consequently, on heating of the irradiated graphite at high temperatures of around 200°C, the annealing of the defects is spontaneous with release of an unusually large energy, called the Wigner energy[5].

Extensive studies have been reported on unirradiated graphite, graphene and carbon nanotubes, including their highly anisotropic elastic[6,7] and thermal-expansion behaviour[8] and spectroscopic studies[9,10] of the phonon spectrum. The macroscopic measurements on irradiated graphite reveal change in the thermal and elastic properties due to damage in the structure[5,11,12]. Neutron irradiation damage of graphite has been studied[13] by high-resolution transmission electron microscopy and Raman spectroscopy. First-principles theoretical studies of the structure, energies and behaviour of defects in graphitic materials has also been reported[14-17]. We note that there is no report of an experimental investigation of the structure of the defects at atomic-level, such as using neutron diffraction. So also, ab-initio simulations of the dynamical behavior of the knocked-out atoms, defect annealing mechanisms and the consequent Wigner energy release are not available. Here we address these aspects using a variety of experimental techniques and first-principles dynamical simulations.

Several graphite samples[18] irradiated with neutrons at various levels of fluence were taken out from a block of irradiated nuclear-grade graphite originally used in the reflector section of the CIRUS research reactor at Trombay, India. The highest fluence of the neutrons encountered by the samples is 2.6×10^{21} neutrons/cm^2 over a period of several decades. The neutron fluence seen by various samples is depicted in Fig. 1. We have also used an

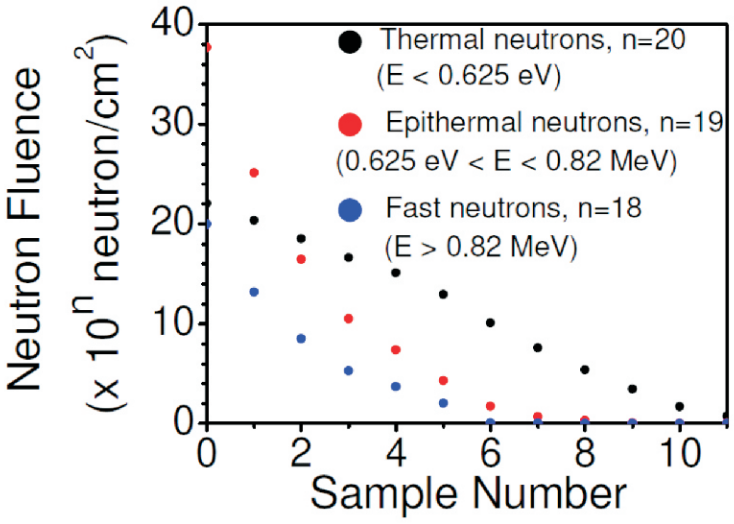

Fig. 1: Neutron fluence as seen by various graphite samples. The irradiated samples are numbered as S0 to S11 in the order of decreasing neutron fluence seen by them; i.e., S0 and S11 have seen the maximum and minimum neutron fluence, respectively. Another unirradiated sample for reference is assigned as sample number S12. The unit (10n neutrons/cm^2) of the vertical axis is different for thermal (n=20), epithermal (n=19) and fast neutrons(n=18)[19] .

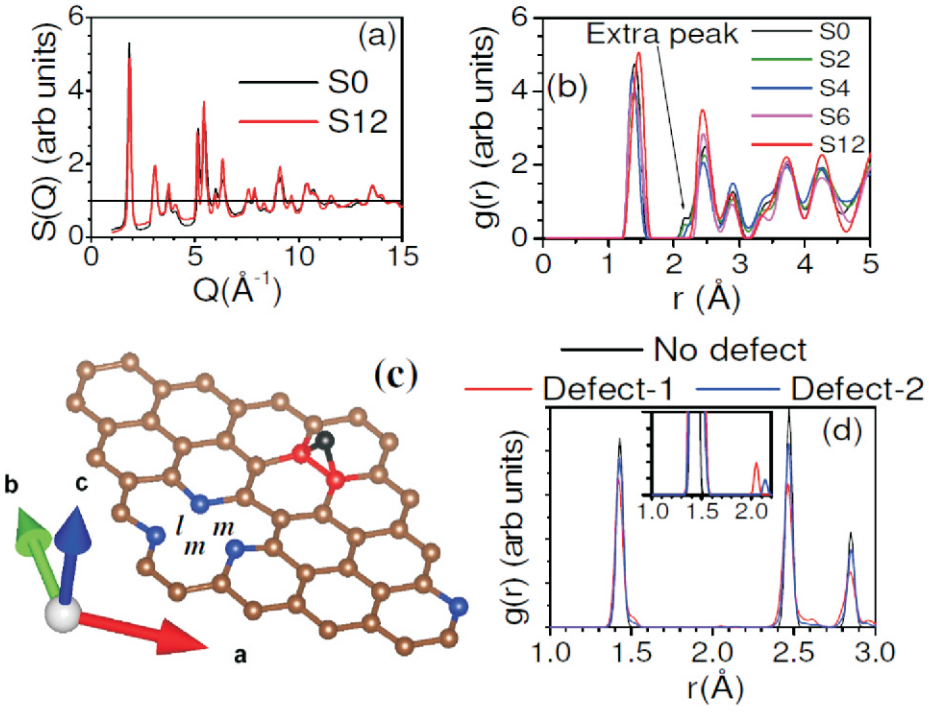

Fig. 2: Topological structures in defected graphite.(a) The neutron diffraction data (S(Q) vs the neutron wave-vector transfer Q) for the un-irradiated (S12) and maximum irradiated (S0) samples. (b) The Pair distribution function of irradiated (S0, S2, S4, S6) and un-irradiated(S12) graphite as obtained from powder neutron diffraction data. (c) A graphite layer with a single Frankel defect in a 4×4×1 super cell. "l" and "m" correspond to the interatomic distance of 2.06 Å to 2.66 Å respectively. The interstitial atom, and the 2-, 3- and 4-coordinated carbon atoms are shown by black, blue, brown and red colors, respectively. (d) The calculated pair correlation functions in the perfect and defected graphite structures. The labels Defect-1 and Defect-2 indicate the defect structures containing a single Frankel defect in 4×4×1 and 4×4×2 supercells, respectively. In the inset, a part of the figure is zoomed.[19] .

unirradiated sample for reference. The samples have been characterized by neutron and X-ray diffraction, differential scanning calorimetry, small angle X-ray scattering, Raman scattering and specific heat measurements, and the details are given in[19] .The results also show that the graphite samples which have been irradiated with very high neutron fluence of epithermal and fast neutrons (exceeding 10^{19} neutrons/cm^2) are highly damaged, while the thermal neutron fluence is not so well correlated. To understand the experimental data on the structure and dynamics, we have performed ab-initio lattice dynamics and molecular dynamics simulations to model the defects, and to identify the mechanisms of annealing of defects in neutron irradiated graphite. While irradiation results in defects at various length scales, our studies have focussed on atomic level defects that are most relevant to the large Wigner energy release.

Topological structures in defected graphite

The experimental neutron diffraction data were obtained using the High-Q powder diffractometer at the Dhruva reactor, and are shown in Fig. 2a. It can be seen that peaks in the diffraction patterns of highly irradiated graphite are broader in comparison to that in the fresh sample. These data are analyzed to determine the real-space pair-distribution function, g(r), which gives the probability of finding neighbors at a distance r. Fig.2b shows the pair distribution function for the unirradiated and several irradiated samples. It is evident from this figure that an additional peak in the g(r) plot of the irradiated samples appears at r=2.17 Å with a redistribution of intensity in the g(r) function. The neutron diffraction results can be understood using ab-initio simulation of the defect structure. As discussed below we find that this peak arises when an atom in the hexagonal layer is knocked-out resulting in a deformed pentagon. The peak at 2.17 Å results from one of the C-C distances in the deformed pentagon from where a vacancy has been created (Fig. 2c).The intensity of the peak at 2.17 Å gradually decreases with decrease of neutron fluence. This provides the experimental evidence for the defect and deformation in the hexagonal structure.

In order to study the defects in graphite we have performed simulation on a 4×4×1

supercell (comprising two graphite layers and 64 atoms) of the graphite structure. Initially one of the carbon atoms in one of the graphite layers was moved in between the two layers, thus creating a vacancy-interstitial pair, also known as a Frenkel defect. The structural relaxation was performed for this configuration. The relaxed structure is shown in Fig. 2c. It can be seen that two of the carbon atoms in the hexagon below the interstitial carbon atom form four-fold coordination due to bonding with the interstitial atom (C-C= 1.40 Å to 1.52 Å). The atom knocked out from a hexagon results in a deformed pentagon structure, in which one of the second neighbor distances of C-C=2.45 Å (in the original hexagon) reduces to 2.06 Å (in the deformed pentagon). Three of the carbon atoms now have 2-fold coordination. The defect structure thus consists of 2-, 3- and 4-coordinated carbon atoms. Further simulations on a larger 4×4×2 (128 atoms) supercell confirmed similar defect structure.

We have plotted the pair correlation function (Fig. 2d) in the perfect and defect structures used in our calculations. We find that the configurations with 1 Frenkel defect in 64 atoms or 128 atoms give an additional peak at about 1.5 Å, which corresponds to the four-fold coordinated carbon atoms. Further, in the g(r) plot we find additional peaks at about 2.06 Å and 2.15 Å in the defect structure with 64 and 128 atoms respectively. As discussed above, these peaks correspond (Fig. 2c) to one of the second neighbor C-C distances in a deformed pentagon as formed due to a vacancy of carbon atoms.

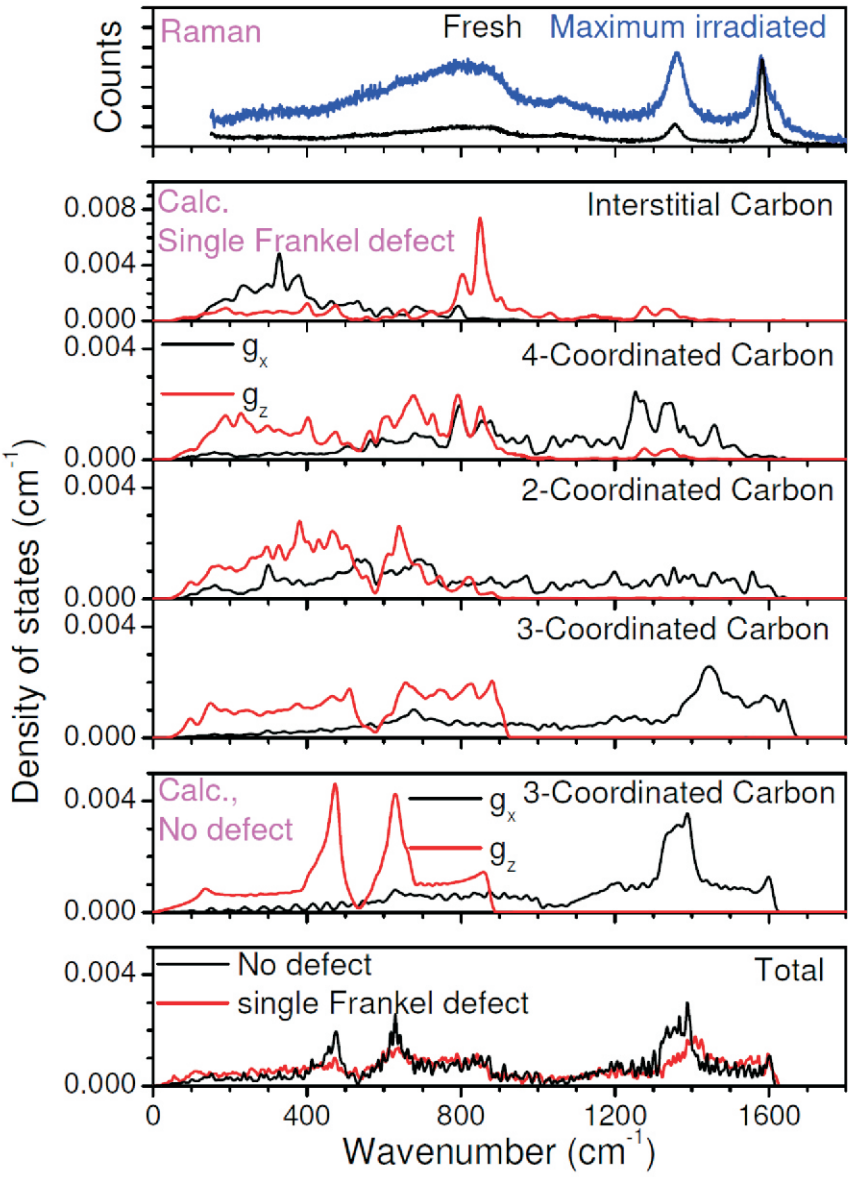

Fig. 3: The measured Raman spectra of the fresh and maximum irradiated graphite sample; and the calculated partial and total phonon density of states of graphite with a single Frankel defect in a 4×4×1 supercell and with no defect. g_x and g_z are the x and z components of the partial phonon density of states respectively[19] .

Phonon spectrum of defected graphite

The measured Raman spectra over 200-1800 cm^{-1} from the fresh and maximum irradiated samples are shown in Fig. 3. It can be seen that the fresh sample shows an intense Raman mode at ~1583 cm^{-1} (G mode), and weak features at around 800 cm^{-1}, ~1355 cm^{-1} (D mode) and ~1620 cm^{-1} ($D_o$mode). For the largest irradiated sample, the intensities of these weak feathers gain very significantly. The intensities of the broad low energy feather around 800 cm^{-1} and the D mode, and also the peak widths increase significantly for the samples irradiated with very high fluence of the epithermal and fast neutrons.

In order to understand the difference in the phonon spectrum at microscopic level we have calculated the phonon density of states as well as the in-plane and out-of-plane partial components of the phonon density of states in both the perfect and the defect structures. As discussed above, the defect structure with the 4×4×1 supercell of graphite has 2-, 3- and 4- coordinated carbon atoms within a graphite layer as well as an interstitial atom in between two layers. We have calculated the partial density of states for each of these types of carbon atoms (Fig. 3).

The changes in the observed Raman spectra (Fig. 3) with irradiation can be understood in terms of the calculated partial phonon density of states of the 2-, 3- and 4- coordinated carbon atoms in the defect structure. We identify (Fig. 3) that the most prominent increase in the intensity of the D-peak at 1360 cm^{-1} is due to the increase in the 4-coordinated carbon atoms. So also, the general increase of the intensity around 800 cm^{-1} may be ascribed to 2- and 3-coordinated carbon defects and the interstitial atom. The results are corroborated by simulations on a single Frankel defect in a 4×4×2 super cell[19] .

Annihilation of defects and release of Wigner energy

The recombination of interstitial atoms and vacancies is the key to the release of Wigner energy in graphite. Earlier calculations[14] showed the stored Wigner energy in a Frankel defect to be about

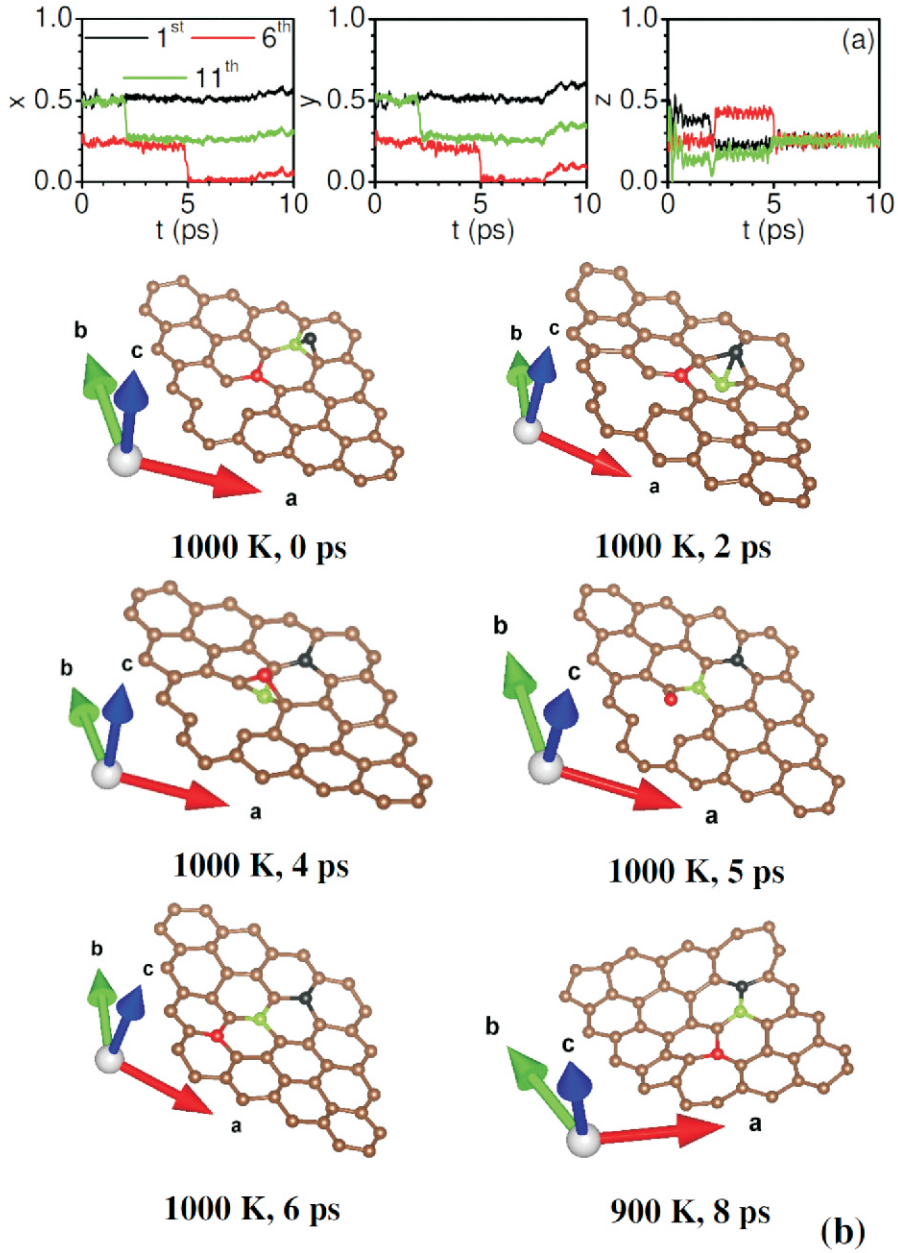

Fig. 4: Annihilation of defects in graphite. Results from ab-initio molecular dynamics simulations in a 4×4×1 supercell with a single Frankel defect at 1000 K.
(a)The time dependence of fractional coordinates of selected three carbon atoms. x, y and z are the fractional coordinate along the a-, b- and c-axis respectively.
(b)The snapshots of atoms in one layer of graphite. A snapshot of partially annealed defect at 900 K is also shown. The selected three carbon atoms are identified as 1st, 6th and 11th in (a) are shown in (b) by black, red and green circles respectively[19] .

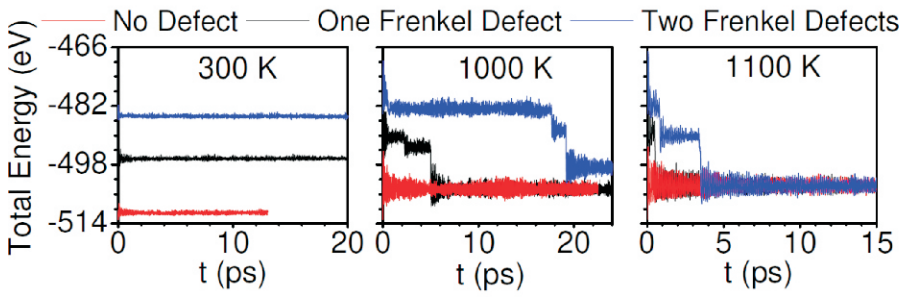

Fig. 5: Annihilation of defects and release of the Wigner energy. The total energy of 4×4×1 supercell (64 atoms) as a function of time with a single and two Frankel defects from ab-initio molecular dynamics simulations[19] .

13-15 eV. The release of Wigner energy[5] in experiments is known to complete at about 650 K. We have verified this in our irradiated samples using Differential Scanning Calorimetry[19]. However our simulation which is performed at a small time-scale of ~200 ps, the temperature for the defect annihilation is expected to be overestimated. However, simulations are useful to understand the mechanism of annealing of defects in graphite.

The simulations are performed on the 4×4×1 supercell with one Frenkel defect at several temperatures from 300 K to 1100 K. The atomic trajectories of carbon atoms have been monitored as a function of time up to 200 ps. Up to 800 K, the defect annihilation process did not start in 200 ps time. However, at 900 K with in 7 ps the interstitial carbon atom moved into the graphite layer. At this time, the defect structure at 900 K (Fig. 4) consists of five- and seven-member carbon rings with in the graphite layer. The structure did not relax further into hexagonal rings in the simulation up to 200 ps.

In the simulation at 1000 K, the defect energy is completely released in two steps as shown by the time dependence of the atomic coordinates. Fig. 4 shows snapshot of atoms at selected times. First at ~2.5ps through a cooperative movement of neighboring carbon atoms we find that the interstitial carbon atom has moved closer to the vacancy. In the second step at ~5.5 ps, the hexagonal structure is restored. The simulations performed at 1100 K showed that within a short time of 1 ps the perfect hexagonal structure is formed. The cascading steps of cooperative movement of atoms represent the pathways of the defect annihilation process. (See Animations in[19], which provide visualization of likely different mechanisms of annealing of defects in multiple steps as discussed above).

We have calculated the total energy of the supercell as a function of time, which reveals the Wigner energy released during the defect annihilation process (Fig. 5). We find the Wigner energy at any temperature to be ~15 eV per vacancy-interstitial defect pair. However, a significant energy barrier prevents the annealing of the defect at a time-scale of 200 ps up to 800 K. However, at 900 K we found that, although the interstitial carbon atom moves in the graphite layer, the structure does not fully anneal in 200 ps time, and still retains a

potential energy of about 5 eV. At 1000 K, the energy of 15 eV is released during the defect annihilation in two steps (Fig. 5), while at 1100 K the same energy is released in a single step.

We have also performed the MD simulations with a structure consisting of two Frankel defects (Fig. 5) in the 4×4×1 supercell. In two Frankel defects the stored Wigner energy is calculated to be ~26.4 eV. We found that at 1000 K one Frankel defect has annealed at ~17.5 ps, while the second Frankel defect is not fully annealed until 100 ps as it forms a pair of five and seven-member rings. However, at 1100 K we found annealing of both the Frankel defects in 4 ps. The annihilation of the first Frankel defect releases about 10-11 eV of energy while that of the second Frankel defect releases about 15 eV. (See Animations in[19]).

Conclusions

In this paper, we have provided direct characterization of defects in neutron irradiated graphite through neutron diffraction, Raman scattering and specific heat measurements, and complemented the results by ab-initio simulations. Specifically, we have observed signatures of 2-, 3- and 4-coordinated carbon topologies around the Frankel defects in both the diffraction and Raman experiments. The microscopic understanding of annealing of defects on heating is achieved through ab-initio molecular dynamics simulations. These involve cooperative movement of atoms in several cascading steps depending on the distance between the vacancy and interstitial positions. The experimental and theoretical work has provided valuable insights in understanding of the structure and dynamical behavior of the defects in neutron irradiated graphite, the annihilation of the defects and consequently release of unusually large Wigner energy.

We note from our ab-initio simulations on various supercells that the defect structure in a graphite layer around a Frankel defect is essentially independent of the separation of such defects along the hexagonal c-axis. This may be expected due to the much weaker van der Waals interaction between the graphite layers compared to the strong covalent bonding within the layers. Other graphitic materials including graphene and carbon nanotubes have similar two-dimensional structure and bonding as in a graphite layer, and these may also be used in high radiation environment including outer space. Therefore, the present work on highly irradiated graphite is of considerable importance to wider areas of graphitic materials.

Acknowledgments

The use of ANUPAM super-computing facility at BARC is acknowledged. SLC thanks the Indian National Science Academy for award of an INSA Senior Scientist position.

Corresponding Author*

Dr. R. Mittal (rmittal@barc.gov.in)

References

[1] IAEA-TECDOC-1521, IAEA, Vienna (2006).

[2] A. Krasheninnikov and F. Banhart, Nature Materials 6, **723** (2007).

[3] J. Lin, Z. Peng, Y. Liu, F. Ruiz-Zepeda, R. Ye, E. L. Samuel, M. J. Yacaman, B. I. Yakobson, and J. M. Tour, Nature Communications 5, **1** (2014).

[4] H. S. Lipson and A. Stokes, Proceedings of the Royal Society of London. Series A. Mathematical and Physical Sciences 181, **101** (1942).

[5] T. Iwata, Journal of Nuclear Materials 133, **361** (1985).

[6] P. De Andres, F. Guinea, and M. Katsnelson, Physical Review B 86, **245409** (2012).

[7] O. Blakslee, D. Proctor, E. Seldin, G. Spence, and T. Weng, Journal of Applied Physics 41, **3373** (1970).

[8] B. Marsden, A. Mummery, and P. Mummery, Proceedings of the Royal Society A: Mathematical, Physical and Engineering Sciences 474, 20180075 (2018).

[9] P. Giura, N. Bonini, G. Creff, J. Brubach, P. Roy, and M. Lazzeri, Physical Review B 86, 121404 (2012).

[10] S. Rols, Z. Benes, E. Anglaret, J. Sauvajol, P. Papanek, J. Fischer, G. Coddens, H. Schober, and A. Dianoux, Physical Review Letters 85, **5222** (2000).

[11] E. Kaxiras and K. Pandey, Physical Review Letters 61, **2693** (1988).

[12] C. Ewels, R. Telling, A. El-Barbary, M. Heggie, and P. Briddon, Physical Review Letters 91, **025505** (2003).

[13] R. Krishna, A. Jones, L. McDermott, and B. Marsden, Journal of Nuclear Materials 467, **557** (2015).

[14] R. H. Telling, C. P. Ewels, A. Ahlam, and M. I. Heggie, Nature materials 2, **333** (2003).

[15] O. V. Yazyev, I. Tavernelli, U. Rothlisberger, and L. Helm, Physical Review B 75, **115418** (2007).

[16] I. Mosyagin, D. Gambino, D. G. Sangiovanni, I. A. Abrikosov, and N. M. Caffrey, Physical Review B 98, **174103** (2018).

[17] P. O. Lehtinen, A. S. Foster, Y. Ma, A. Krasheninnikov, and R. M. Nieminen, Physical Review Letters 93, **187202** (2004).

[18] R. Ranjan, S. Bhattacharya, P. V. Varde, C. G. Karhadkar, P. Mandal, M. K. Ojha, G. K. Mallik, and V. D. Alur, BARC Report (External) **BARC/2017/E/006**.

[19] R. Mittal et al, Physical Review B 102, **064103** (2020).